6.

DESIGN AND ANALYSIS OF PLANAR MONOPOLE MIMO/DIVERSITY ANTENNA FOR LTE MOBILE HANDSETS

6.1 Introduction

In recent years, Long Term Evolution (LTE) technology came in the front line of fourth generation (4G) mobile communications. As one of the key techniques in LTE, Multiple Input Multiple Output (MIMO) technology attracts significant attention of the researchers. The MIMO and diversity systems are potential technologies for enhancing the performances such as system reliability, channel capacity, and data transmission rate. It is because the MIMO system supports multiple independent channels at both transmitting and receiving sides to offer improved capacity over single antenna topology without using extra radiated power and spectrum bandwidth [Foschini (1998)].

So in view of the above, researchers are focussing on the LTE technology with MIMO implementation. There are some studies have been carried out to achieve LTE band with MIMO antenna configuration [Lee *et al.* (2014), Lee *et al.* (2011), Baek and Choi (2014), Yu *et al.* (2010), Kim *et al.* (2012), Park *et al.* (2009), Thomas *et al.* (2012), Wong *et al.* (2011), Zhang *et al.* (2013)]. To obtain LTE 13 band, a closely mounted PIFA in conjunction with a T-shaped common radiator was proposed [Lee *et al.* (2014)]. But the overall volume of the PIFA is not favourable for slim mobile handset due to its non-planar structure. In [Lee *et al.* (2011)], LTE MIMO antenna designed over ferrite substrate, which causes the excitation of surface wave that leads to lower radiation efficiency and gain. The folded technique applied to miniaturize the antenna element and to accomplish the LTE band with small form factor [Baek and Choi (2014), Yu *et al.* (2010)]. But the geometry of the antenna becomes non-planar which is not suitable for the slim handsets. In [Kim *et al.* (2012)], meandered line technique used to achieve compactness of the antenna. But the thickness of the antenna attained certain

height, due to which the planar nature of the antenna is disturbed. A quad band mobile handset antenna presented for LTE700 MIMO application [Park *et al.* (2009)], but whole antenna system deposed on the one side of the PCB board which make larger form factor as well as antenna was designed over a carrier which will bring the difficulties during the fabrication process.

Further, the LTE/WWAN band with multiple antenna configurations were reported in [Thomas *et al.* (2012), Wong *et al.* (2011), Zhang *et al.* (2013)], which used coupled-fed antennas to get lower band and wide upper bands. But to make the compact structure, the antenna was folded at the edges of the strips which provide 3D geometry which bestows difficult fabrication steps. The chip inductor was used in the design of antennas to minimize the physical length required for desired resonant modes which produces losses and increases fabrication process. All the above constraints are restricting the implementation of these antennas in modern day mobile handsets.

Somehow, multiple antennas within the limited space of mobile phones were implemented successfully. But mutual coupling between closely packed antenna elements is one of the key challenges. So, the most important recent issue is how to design compact MIMO antennas at lower frequency bands and how to obtain sufficient isolation and low envelope correlation coefficient (ECC) between closely placed antennas in portable MIMO-embedded devices. Some of the aspirant isolation techniques reported in [Diallo *et al.* (2006), Meshram *et al.* (2012), Chen *et al.* (2008), Zhang *et al.* (2010)] to enhance the isolation between antenna elements. Several kinds of decoupling techniques were readily available, such as neutralization line technique [Diallo *et al.* (2006)], etching slots [Meshram *et al.* (2012)], decoupling circuit [Chen *et al.* (2008)], by exciting new resonant mode [Zhang *et al.* (2010)], that utilizes the edges of two PIFAs as well as another slot cut on the ground plane to form a half-wavelength U-shaped slot in-between, and protruded ground plane [Ban *et al.* (2014a), and Ban *et al.* (2014b)]. However, neutralization strip, etching slots usually introduce some complex well tuned metal structures, which leads to additional area consumption. Furthermore,

decoupling circuit was often used for the single and narrowband decoupling, which is not so applicable for wideband decoupling. The excitation of new resonant mode can not be utilized for a ground plane with arbitrary size and shape (e.g. that of a mobile phone) because it may not be possible to match the decoupling slots well enough to excite the modes successfully. The area taken by protruded ground plane in [Zhang *et al.* (2010), Ban *et al.* (2014)] was large e.g. space is not left for the speaker, microphone or other electronics component which can be set into the mobile handset near to the antenna element.

Moreover, the trend for mobile terminals is towards smaller and thinner sizes, increasing number of operating frequency bands, and improved transmit and receive performance. Thus, one important challenge lies in implementing MIMO antenna that are closely spaced in a compact handset. An additional challenge is the unavoidable interaction with the user. The mobile phone generally used in close proximity of user body, which reduces received power at the mobile terminal. The amount of power received from mobile base station to mobile user depends not only on the factors related to mobile phone but also of antenna design. The body loss (ratio of efficiency with and without user body) is significantly depending on the antenna design for mobile phones. The antenna characteristics such as impedance matching, radiation efficiency, and radiation pattern are affected by the presence of the objects, especially presence of user in the vicinity of the antenna.

Some of the mobile terminal antennas studied in the presence of human head and hand [Gao *et al.* (2013), Yu *et al.* (2010), Pelosi *et al.* (2010), Iivonen *et al.* (2011), Holopainen *et al.* (2011), Li *et al.* (2009)]. Unfortunately, the researchers in [Gao *et al.* (2013), Yu *et al.* (2010), Pelosi *et al.* (2010), Iivonen *et al.* (2011), Holopainen *et al.* (2011), Li *et al.* (2009)], focussed only on the user effects on a single antenna element. Further, diversity antennas proposed by some of the authors along with the study of their performances in the user proximity [Plicaic *et al.* (2008), Buskgaard *et al.* (2014), Zhang *et al.* (2013), Plicanic *et al.* (2009)]. [Plicaic *et al.* (2008), Buskgaard *et al.* (2014), Zhang *et al.* (2013), Plicanic *et al.*

(2009)], in which multi band diversity antennas analysed in the presence of user (Only hand considered). An adaptive quad element multi wideband antenna array for user effective LTE MIMO mobile terminal was proposed by Zhang *et al.* [Zhang *et al.* (2013)]. But there are four elements considered over the mobile circuit board during the performance study, which leads to the complex situation when implemented within the real scenario of mobile phones. In [Plicanic *et al.* (2009)], authors' discussed about diversity performances such as actual diversity gain (ADG), diversity gain (DG), and effective diversity gain (EDG) in the user proximity. This study was carried out on fixed single position of antenna over mobile circuit board therefore it is very difficult to say about its performances. So, consideration of same antenna with different location over mobile circuit board would be more convenient during its performances study. Then with the help of diversity parameters, radiation performances, multiplexing efficiency, and specific absorption rate (SAR), we can decide the suitable location of MIMO antenna elements over the circuit board.

In this chapter, a planar, printed MIMO antenna for slim mobile handset is demonstrated. The dual-antenna system comprises of two symmetrical antenna elements, printed on PCB of mobile phone. Each antenna element consists of coupled-fed loop antenna. The loop antenna is formed by a quarter wavelength (at 762 MHz) meandered loop strip with end terminal short-circuited to the ground plane. A T-shaped protruded ground is deliberately designed to enhance the impedance matching and decoupled the two closely deposed antenna elements (distance between antennas elements are 0.03λ at 762 MHz). The integrity of the T-shaped decoupling structure and coupled-fed loop antenna array covers LTE700 (0.747 GHz – 0.787 GHz) and WWAN (1.7 GHz – 3.04 GHz) bands based on -6 dB reflection coefficient and achieved isolation between elements well below -10 dB over all the operating bands. The application platform is LTE700, GSM1700, GMS1800, UMTS, Wi-Fi, Bluetooth, LTE2300, and LTE2500 bands for the 2G/3G/4G mobile terminals. The effect of user proximity by considering the actual mobile environment is also studied in the form of total radiated power (TRP), specific absorption rate (SAR), diversity performances, and radiation

performances. Finally, a prototype is fabricated and tested with network analyser. The measured results are found in good agreement with simulated results. Further, the effect of user's body on the performance parameters of planar monopole MIMO antenna is studied by placing the antenna elements at top as well as bottom of the mobile circuit board. Three different commonly used configurations namely, SAM head and PDA hand (Talk mode), PDA hand (Data mode), and Dual hand (Read mode) are considered for this study. The *S*-parameters, diversity parameters, SPLSR, and TRP are calculated in the user proximity.

6.2 Antenna Configuration and Design

Fig. 6.1 shows the front and rear view of the proposed MIMO antenna. It consists of two symmetrical planar antennas on front side (no ground plane on the rear side in this area) of low cost FR4 substrate (thickness is 0.8 mm) of dielectric constant (ε_r = 4.4) and loss tangent (tan δ = 0.018). Each array element is connected to a 50Ω coaxial connector to excite the antenna, with point A_1 and A_2 serving as feed points and point B_1, B_2 serving as PCB shorting points. The rear view of the proposed antenna consists of protruded T-shaped ground plane which is used to enhance the isolation as well as impedance matching at higher frequency bands. The details of T-shaped protruded ground plane are given in Fig. 6.1(a). Two capacitive coupled-fed shorted loop antennas are closely mounted with the separation of 12 mm (0.03λ at 762 MHz). The detailed dimensions of the proposed shorted loop antenna are shown in Fig. 6.1(b). The fabrication of the prototype is done on T-Tech QC-5000 prototyping system which is shown in Fig. 6.1(c).

To illustrate the design and mechanism of the proposed antenna, reflection coefficient and vector surface current distributions are shown in Fig. 6.2. The evolution starts from the driven element and proceed towards the proposed configuration to achieve the desired goal. Initially, driven element is designed to excite the main shorting strip loop antenna. The electrical length of driven strip is λ/4 at 1.865 GHz (≅ 40.5 mm) and antenna resonates at 1.86 GHz corresponding to this electrical length as shown in Fig. 6.2(a) and vector surface current [Case 1,

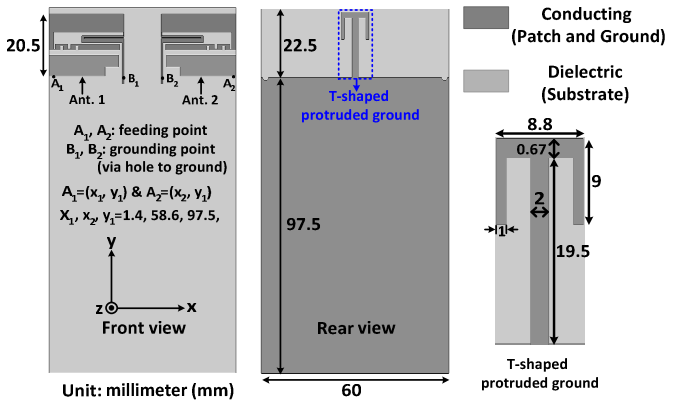

(a)

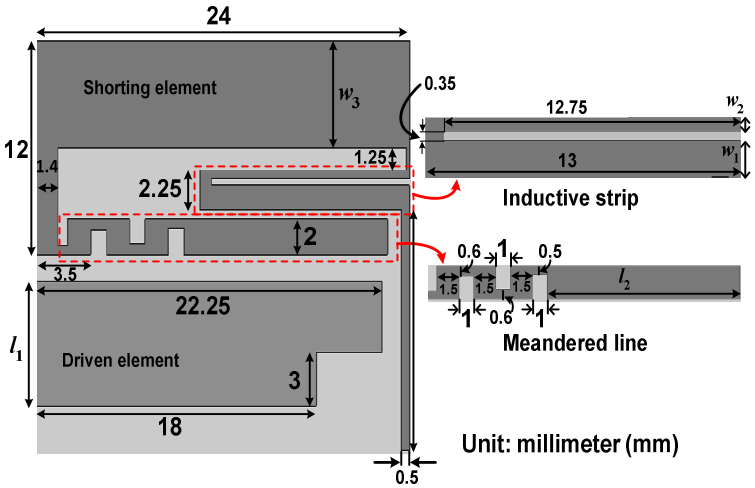

(b)

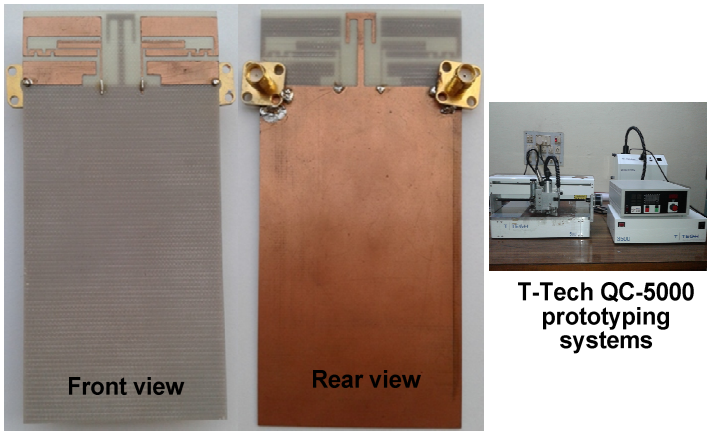

Fabricated prototype

(c)

Figure 6.1: (a) Front and rear view of the proposed antenna, (b) Detailed dimensions of the single antenna element, and (c) Fabricated prototype.

1.865 GHz] starts travelling from feed point to outer boundary of the driven element (covers distance λ/4 at 1.865 GHz) which is responsible for 1.86 GHz resonance as shown in Fig. 6.2(b). In order to achieve the lower operating band and wideband operation at higher frequency band, quarter wave inductive strip is designed and driven element is used as coupling feed, respectively. The current distribution [Case 2, 1.01 GHz] provides further explanation about the resonance mode at lower resonance frequency for the Case 2. The coupling between driven element and shorted loop strip provides wideband at higher frequency whereas lower resonance occurs due to increased electrical length of the shorted strip which is clearly depicted in Fig. 6.2 [dashed line shows current path in Fig. 6.2(b)]. Further, to achieve lower resonance around LTE700 frequency band as well as to maintain compactness of the antenna, meandered line structure at the end terminal of the shorting strip is used. Due to addition of the meandered line structure, the lower resonance shifted from 1.01 GHz to 0.861 GHz but LTE700 frequency band is still not achieved. The occurrence of resonance at 0.861 GHz is due to the quarter wavelength of the meandered shorting strip. The current [Case 3, 0.86 GHz] on the meandered shorted loop antenna starts flowing from coupling point to the end of meandered line which also confirms the resonance at 0.86 GHz. Finally, to get the desired goal, combination of meandered line and inductive strip are shorted with ground through via. With the combination of meandered line and inductive strip, total electrical length of the shorted loop antenna is increased and resonance occurs at 0.767 GHz corresponding to the quarter wavelength of the shorting strip. After optimization of all the shape parameters, antenna resonates at 0.767 GHz, 1.813 GHz, and 2.95 GHz which covers the LTE700, GSM1700, GMS1800, UMTS, Wi-Fi, Bluetooth, LTE2300, and LTE2500 operating bands with below -10 dB isolation over all the operating bands.

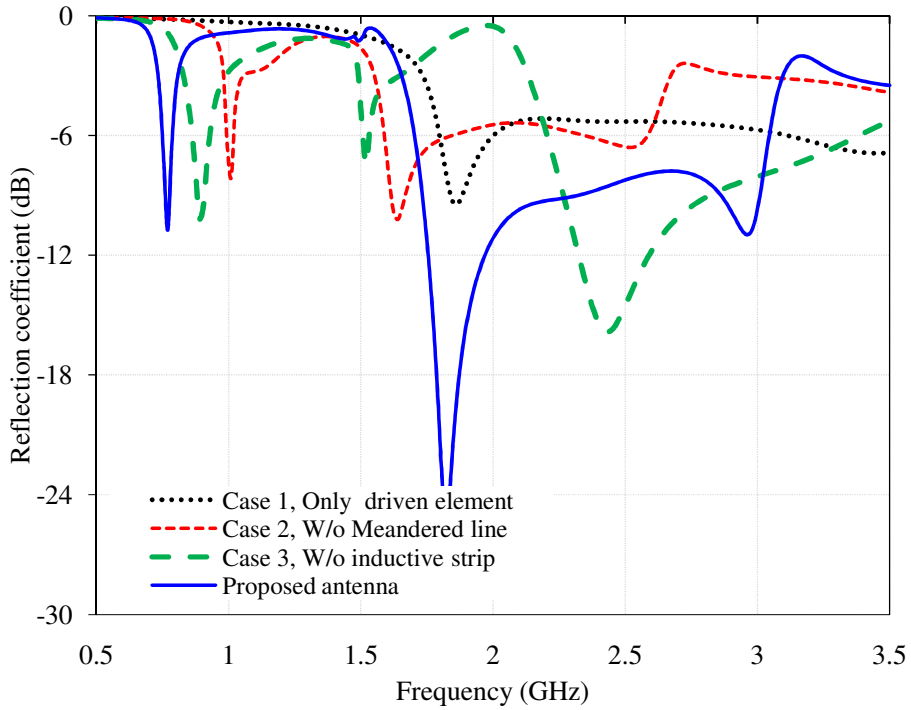

(a)

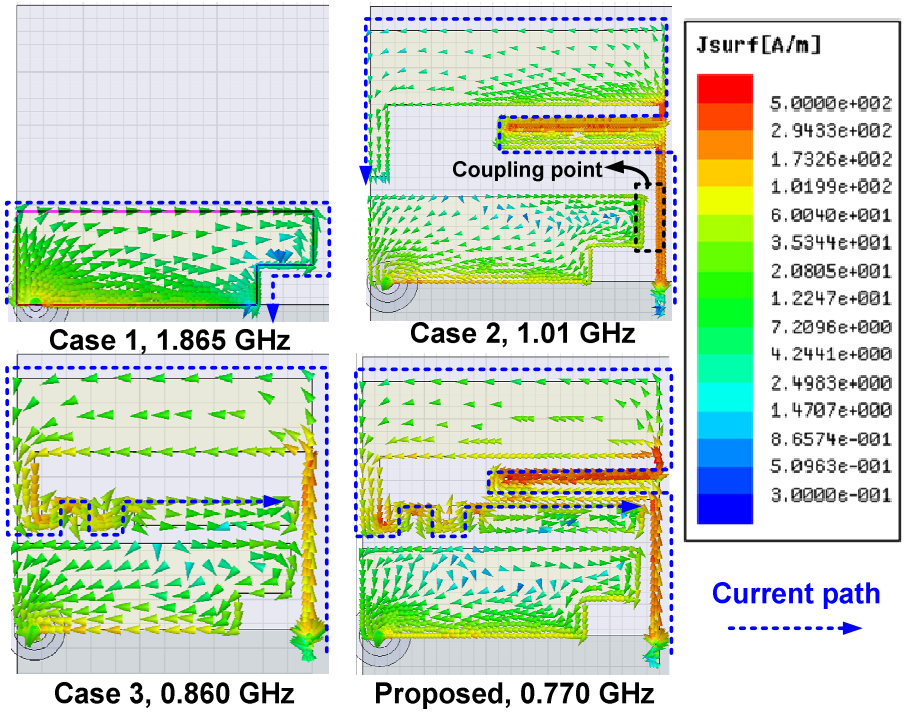

(b)

Figure 6.2: (a) Effect of different configurations on reflection coefficient, (b) Surface current distribution for different cases.

6.3 Results and Discussion

All the shape parameters of the proposed antenna is optimized using Ansoft's High Frequency Structure Simulator (HFSS) and before going for fabrication, optimized antenna is also simulated using Computer Simulation Technology Microwave Studio (CST MWS). Further, CST MWS is used to evaluate the radiation performances, diversity performances, and to study the effect of user proximity.

6.3.1 *S*-parameters and Radiation Performances

6.3.1.1 Parametric Analysis

Some of the key parameters of the proposed antenna are optimized to get the proper resonance frequency so that antenna can operate over desired application platform. All the optimization of the shape parameters are carried out using Ansoft's simulation software.

In order to this, vertical length of the driven element is optimized. The variation of reflection coefficient due to the vertical length of the driven element is shown in Fig. 6.3(a), respectively. It is observed that when l_1 increases, higher cut off frequency of higher operating frequency band shifts towards higher and lower operating frequency shifted towards higher frequency side. To obtain the desired resonance and operating bands, vertical length (l_2) of the driven element is 7mm.

Further, shape parameters of the shorted radiating element are optimized. The combinations of inductive and meandered line are responsible for the LTE frequency band and WWAN band. Since, the width of the inductive strip and length of the meandered line are crucial parameters to tune the lower operating bandwidth. Therefore, to optimized lower operating frequency band, the width and length of the elements of the shorted radiating elements are chosen. The effect of width of the inductive strip on reflection coefficient is shown in Fig. 6.3(b) and (c). When width (w_1 and w_2) of the inductive strip increases, lower resonance frequency slightly shifted towards lower frequency side whereas little deterioration at higher frequency is observed. The trade-off value of strip width w_1 and w_2 are 1.4mm and 0.5mm, respectively.

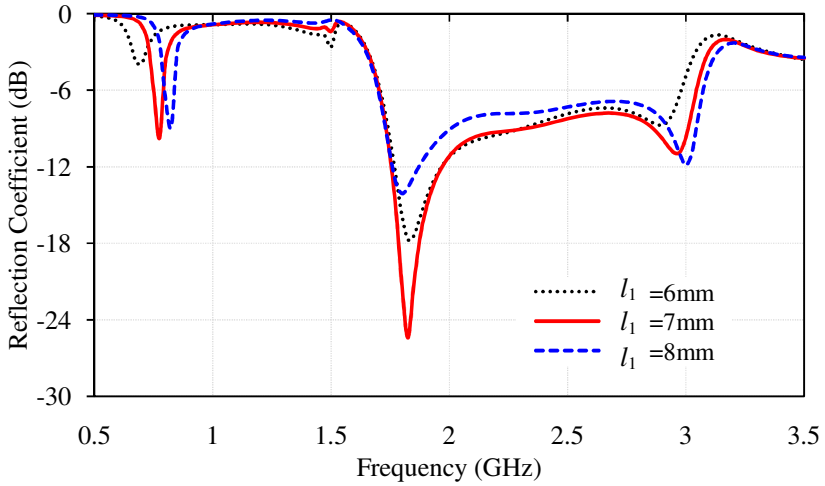

(a)

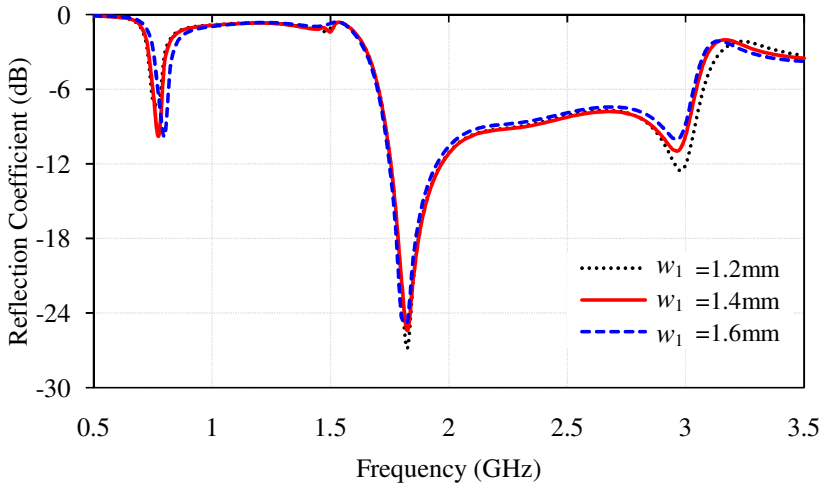

(b)

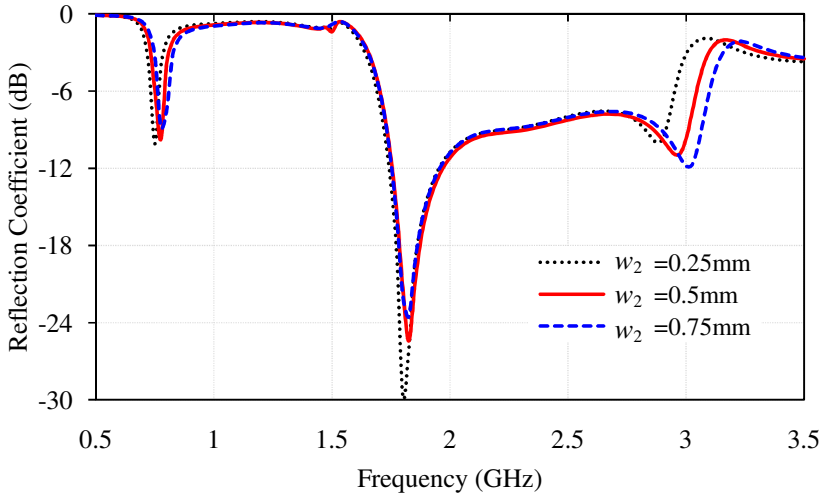

(c)

Figure 6.3: Variation of reflection coefficient with various shape parameters (a) l_2 (b) w_1, and (c) w_2.

Further, parameter w_3 tuned to get the desired operating frequency band and variation is shown in Fig. 6.4(a). It is observed that when w_3 increases lower resonance shifted towards lower side due to increase of the electrical length and simultaneously impedance matching deteriorated at higher operating band. The optimum value of w_3 is 6mm for which the desired operating frequency bands cover. The length l_2 of the end terminal of the meandered line is optimized to tune the operating frequency band. The effect of l_2 similarly affect the lower resonance frequency as w_3 but the lower cut off frequency of higher frequency band shifted towards lower side. The trade-off value of l_2 to get the desired operating band is 13.1 mm as shown in Fig. 6.4(b).

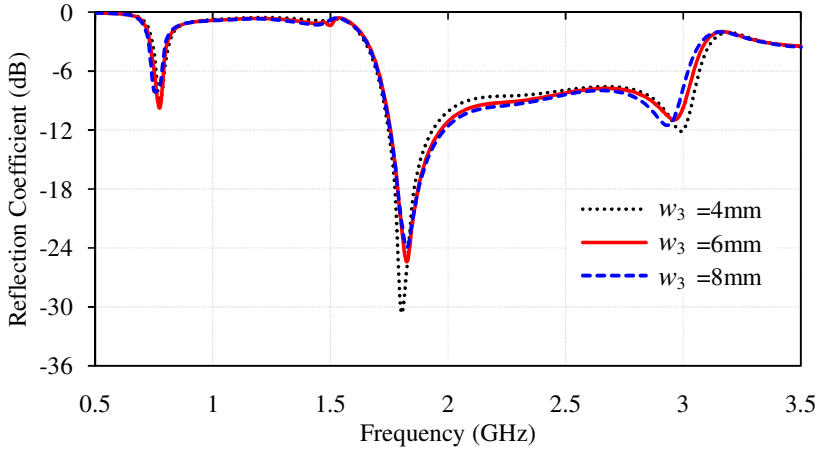

(a)

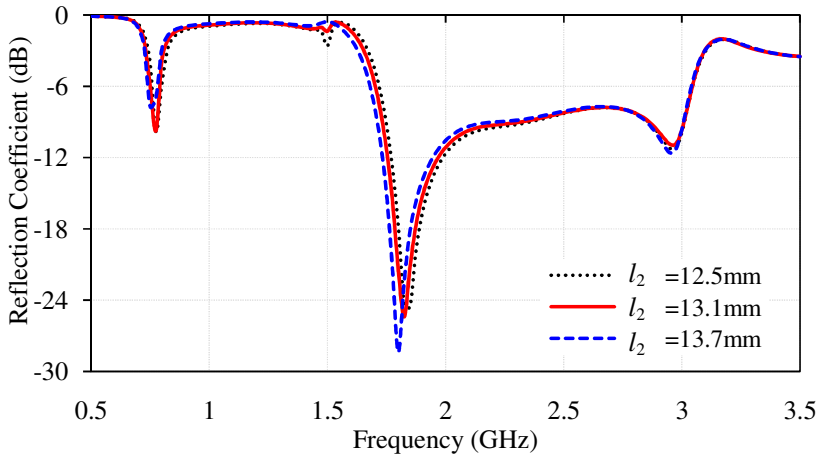

(b)

Figure 6.4: Variation of reflection coefficient with various shape parameters (a) w_3, and (b) l_2.

To study the effect of protruded ground plane, *S*-parameters are shown in Fig. 6.5. It is observed that without protruded ground plane, isolation at higher frequency side is less than -10 dB especially at two resonances i.e., 1.68 GHz and 2.84 GHz. Apart from these two resonances, isolation is well below -10 dB. So it is required to enhance the isolation at higher frequency side especially at two higher resonances while the isolation at lower frequency side is maintained well below -10 dB. The isolation is significantly enhanced at higher frequency band for the proposed antenna with the T-shaped protruded ground plane and improvement in impedance matching is also observed at higher frequency band. The effect of protruded ground plane play significant role in isolation enhancement at higher frequency whereas insignificant role at lower frequency. This is because of the length of protruded ground (T-shaped) is λ/4 which is corresponding to the higher frequency i.e., 2.45 GHz.

6.3.1.2 Simulated and Measured *S*-parameters

After the optimization of shape parameters of the proposed planar monopole antenna, the antenna is fabricated by using T-Tech QC-5000 prototyping system. Further, the fabricated prototype is measured by Anritsu VNA Master MS2038C

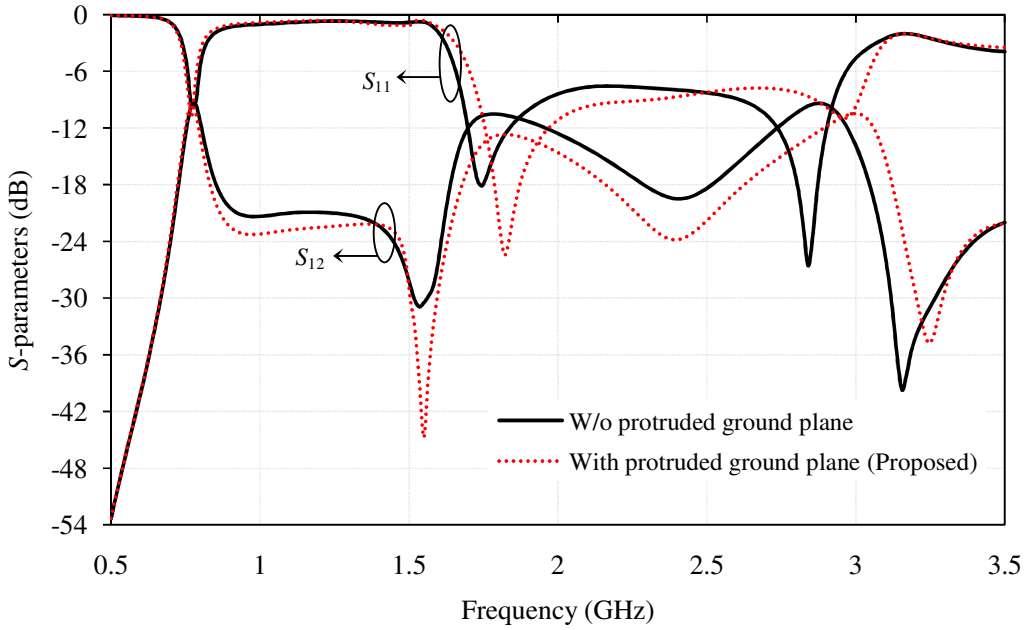

Figure 6.5: Effect of protruded ground plane on *S*-parameters.

(5 KHz – 20 GHz). The simulated and measured *S*-parameters are shown in Fig. 6.6. Some discrepancies between simulated and measured results are observed which is due to manufacturing tolerances. The proposed antenna array covers LTE700 (0.747 GHz – 0.787 GHz) and WWAN (1.7 GHz – 3.04 GHz) based on -6 dB reflection coefficient and achieved isolation between elements well below -10 dB over all the operating bands. The application platform is LTE700, GSM1700, GMS1800, UMTS, Wi-Fi, Bluetooth, LTE2300, and LTE2500 bands for the 2G/3G/4G mobile terminals.

6.3.1.3 Radiation Performances

The simulated 3D far field and measured 2D far field radiation patterns of the proposed antenna array at different frequencies i.e., 0.77 GHz, 1.9 GHz, and 2.5 GHz are achieved by exciting a single port at a time and matched terminated to other ports and are shown in Fig. 6.7(a) and (b), respectively. It illustrates that the simulated and measured radiation patterns of the two elements point to complimentary spatial region which shows pattern diversity criterion of the proposed antenna and this property can provide low correlation and good antenna diversity in free space. Fig. 6.8 shows the calculated total antenna efficiency by

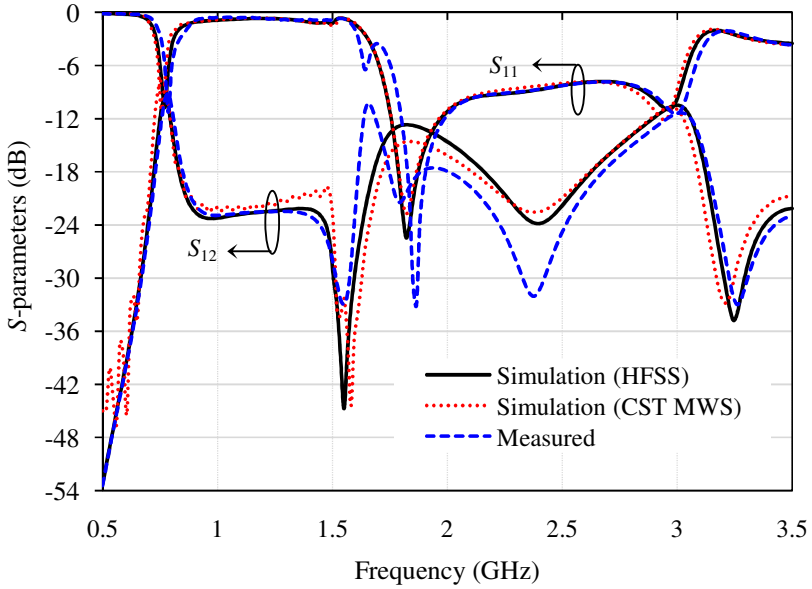

Figure 6.6: Simulated and measured *S*-parameters of the proposed planar monopole MIMO antenna.

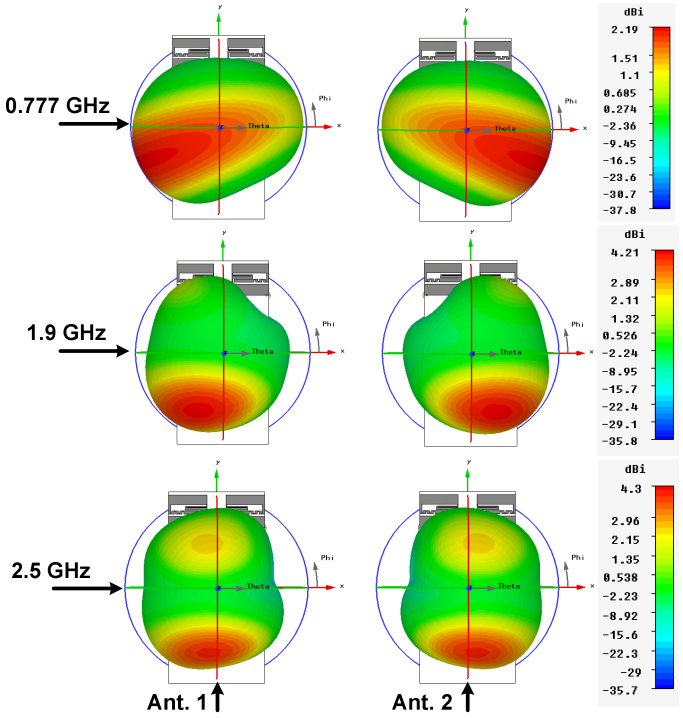

(a)

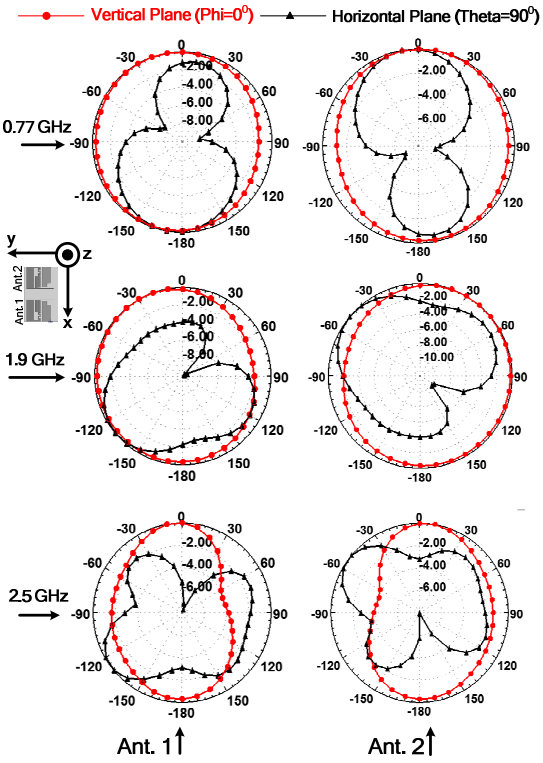

(b)

Figure 6.7: (a) Simulated 3D and (b) Measured 2D far field radiation patterns at 0.777GHz, 1.9GHz, and 2.5GHz.

considering the reflection losses for the proposed antenna in free space. Ant. 1 and Ant. 2 are identical and symmetrically placed on PCB of mobile circuit board. So total antenna efficiency is almost same for each antenna elements in free space and efficiency at port are given here. It is noticed that total antenna efficiency varies in LTE700 frequency band from 43% to 51% and 57% to 90% in WWAN frequency band. Also, the variation of peak realized gain is shown in Fig. 6.8. It is noticed that the variation of measured peak realized gain between -0.86 dBi to -1.7dBi in LTE700 frequency band and -2dBi to 1dBi in WWAN frequency band.

6.3.2 Diversity Parameters Analysis in Free Space

The ECC, MEG, EDG are most important parameters for evaluating the diversity performances of the proposed antenna. The calculation of the diversity parameters are carried out by using CST MWS.

The ECC is calculated using far field pattern data by considering the antenna system lossy structure and uniform scattering environment. The ECC is calculated similarly to the previous chapters and given in Table 6.1. It is observed that the values of ECC are well below the allowable limit 0.5.

Further, MEG is calculated according to the given formula (section 2.3.1). The calculated values of MEGs are given in Table 6.2 for different values of XPR. It is

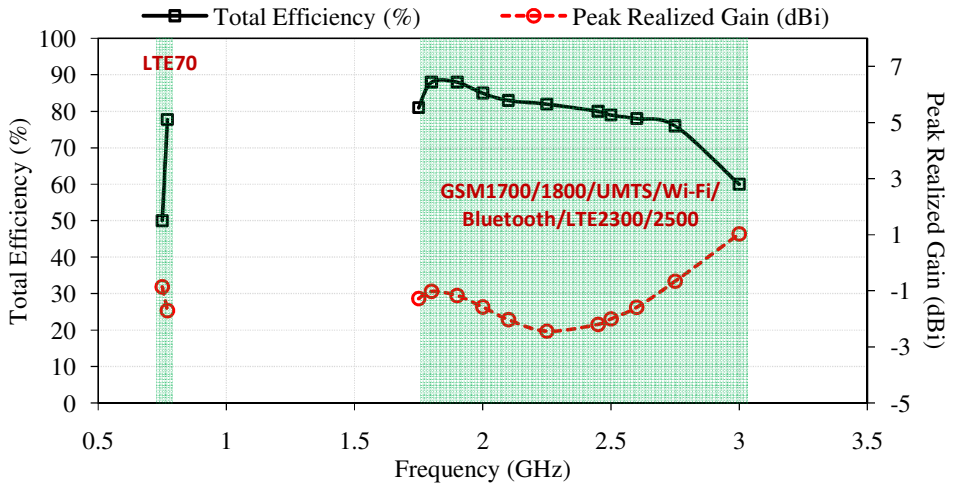

Figure 6.8: Variation of calculated total efficiency and measured peak realized gain with frequency.

observed that MEGs are equal for both antennas and ratio of MEGs are close to unity, which satisfy the equality criterion for the two antennas.

The next important diversity parameter is EDG. The apparent diversity gain which is based on selection combining w.r.t. 1% distribution level does not include the antenna efficiency. So we cannot achieve effectiveness of diversity capability without considering antenna efficiency into account. In view of this, here we calculated the effective diversity gain (EDG). The calculated values of EDG are given in Table 6.1.

6.4 Performances Study of Planar Monopole MIMO Antenna in User Proximity with Mobile environment

6.4.1 Simulation Setup and Configurations

Further, to consider real scenario, a typical hand held geometric model is shown in Fig. 6.9(a), which is based on the near field environments. The mobile environment comprises of large size touch screen LCD ($72 \times 53 \times 2$ mm^3), battery ($64 \times 46 \times 3$ mm^3), camera (diameter is 17 mm and thickness is 6.5 mm), and speaker ($18 \times 1 \times 1.8$ mm^3). A large size LCD and battery are settled parallel with spacing of 1mm and are connected with the main PCB via connectors. To maintain the thinness of the mobile devices, planar antenna is considered. Due to which, LCD is placed within the ground portion. Beyond the ground, antenna portions are overlapped by the LCD screen resulting in antenna performance

Table 6.1: Diversity performance of the proposed planar monopole MIMO antenna.

Frequency (GHz)	ECC	Effective Diversity Gain (1%) (dB)
0.777	0.427	3.85
1.8	0.012	8.83
1.9	0.002	8.84
2.1	0.0004	8.31
2.5	0.0003	7.9

Table 6.2: MEG at different frequencies of planar monopole MIMO antenna.

Frequency (GHz)	Indoor (XPR=5 dB)		Outdoor (XPR=1 dB)		Isotropic (XPR=0 dB)	
	MEG1	MEG2	MEG1	MEG2	MEG1	MEG2
0.777	-9.4	-9.4	-7.3	-7.3	-6.8	-6.8
1.8	-7.6	-7.6	-5.8	-5.8	-5.3	-5.3
1.9	-7.4	-7.4	-5.6	-5.6	-5.1	-5.1
2.1	-7.3	-7.3	-5.5	-5.5	-5.11	-5.11
2.5	-7.5	-7.5	-5.9	-5.9	-5.46	-5.46

deteriorated. By the trade-off between simplicity of the antenna structure and size of LCD, the MIMO antenna is placed on the one top corner of the substrate which is off-display area while the large size LCD display is placed opposite side of the substrate. A camera and speaker are placed same side of the PCB (on the side of antenna elements). These components are near to the antenna elements and deposed in the available space. All these components are considered as perfect electric conductor (PEC) during simulations. The small metallic components like two buttons and one microphone are also considered which are far from antenna elements. All these mobile components and antenna elements are covered with a 1 mm thick plastic box of dielectric constant 3.0 and conductivity 0.02 S/m which form housing of the mobile phone. The simulation setup of mobile environment is created in CST MWS. The effect of near field mobile environment on *S*-parameters is shown in Fig. 6.9(b). It is observed that significant effect of the mobile environment is observed on the reflection and coupling *S*-parameters. It is interestingly noted that at lower frequency, both impedance matching as well as isolation level improved. This is due to the placement of the speaker near to the antenna element which acts as reflector for antenna elements. Due to the placement of speaker near the T-shaped protruded ground plane, electrical length of the T-shaped protruded ground increases by the capacitive coupling between T-shaped structure and speaker and hence improved isolation is observed in the presence of mobile environment.

Further, user's body is placed near to the mobile phone (antenna with mobile environment) and position of whole mobile phone and user body [SAM head and PDA hand (Talk mode); PDA hand (Data mode)] is in accordance with the Cellular Telecommunication Industry Association (CTIA) [CTIA Report (2011)]. Generally, users use the mobile phone in three different ways i.e. Talk mode, Data mode, and Dual hand (Read mode). For the case of dual hands, since there is no standard yet, the whole antenna array and dual hands are arranged in a common handsets-holding way. The dielectric properties of the head and hand tissue can be found in [CTIA Report (2011)] and given in Table 6.3. Since the antenna elements placed symmetrical on the mobile circuit board, using the left or right hand will not cause any difference. In the simulation, we assume that the user uses the right hand (as most people do). In order to study, the effect of antenna location on mobile circuit board we consider two different locations over mobile circuit board i.e. top and bottom for the each case of user proximity. We refer to the antenna close to the ear as top antenna and the one close to the mouth as bottom antenna.

All the simulations setup for the study of user proximity is created in CST MWS. The tissue model and antenna with mobile phone configuration in Talk mode is shown in Fig. 6.10(a). In Fig. 6.10(b), the tissue model and antenna locations are presented for the Data mode. The hand model and holding rules are exactly the same as in the Talk mode. The Read mode is shown in Fig. 6.10(c).

Table 6.3: Dielectric properties of the human head and hand tissues.

Frequency (GHz)	Human Head Tissue		Human Hand Tissue	
	ε	σ (S/m)	ε	σ (S/m)
0.75	42.5	0.88	32.2	0.51
1.8	40	1.4	27	0.99
1.9	40	1.4	26.7	1.04
2.1	39.8	1.49	26.3	1.14
2.45	39.2	1.8	25.7	1.32

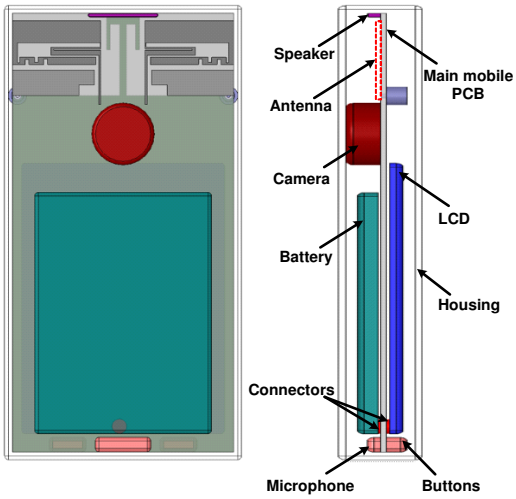

(a)

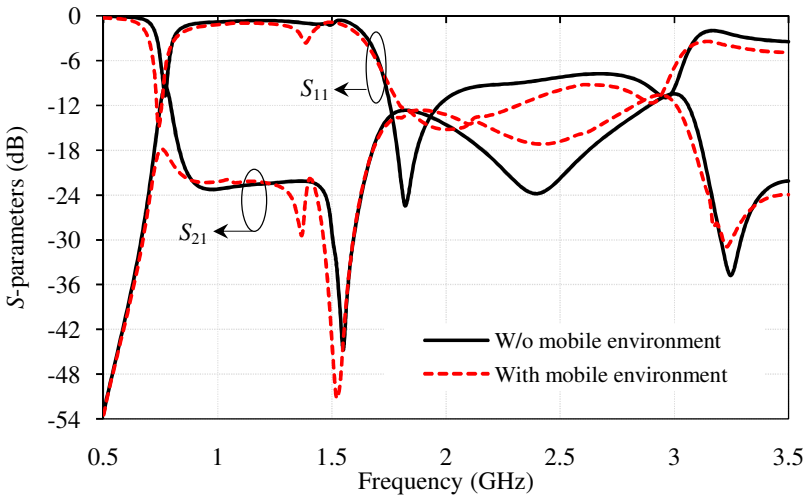

(b)

Figure 6.9: (a) Actual mobile environment with antenna elements and (b) Effect of mobile environment on *S*-parameters.

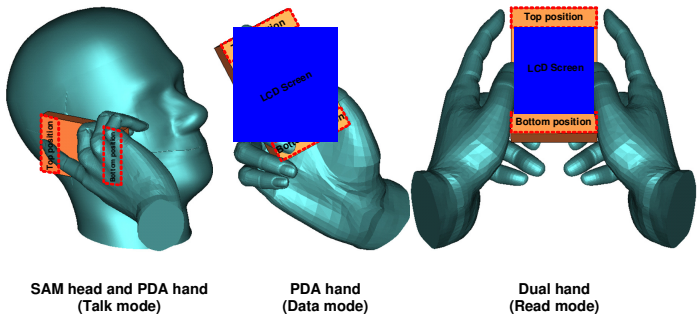

(a) (b) (c)

Figure 6.10: Model of antenna elements locations of (a) SAM Head and PDA Hand (Talk mode), (b) PDA Hand (Data mode), and (c) Dual Hand (Read mode).

6.4.2 *S*-parameters Analysis

The antenna is designed and tested successfully in the free space for LTE700 (0.747 GHz – 0.787 GHz) and WWAN (1.7 GHz – 3.04 GHz) applications based on -6 dB reflection coefficient in previous sections. The isolation between elements are well below -10 dB over all the operating bands in free space and results are given in the above section. The designed antenna provides the application platform LTE700, GSM1700, GMS1800, UMTS, Wi-Fi, Bluetooth, LTE2300, and LTE2500 bands for the 2G/3G/4G mobile terminals.

Further, to verify the robustness of the antenna performances in the user proximity, initially *S*-parameters are studied for two different position of the antenna on mobile circuit board i.e. antenna at top position and bottom position. For the Talk mode, variation of *S*-parameters is shown in Fig. 6.11(a). It is observed that, when antenna is located at the top of the mobile circuit board the reflection coefficient of Ant. 1 and Ant. 2 is well matched at lower as well as higher frequency bands which helps to cover the desired application bands. But, bottom located antenna element especially Ant. 2 shows poor impedance matching at lower frequency band and acceptable matching at higher frequency bands. So, it can be concluded that bottom located antenna element is not achieved the desire application bands because reflection from human head leads deteriorate in impedance matching of antenna elements. Whereas, isolation for top located antenna elements is well below -10 dB for lower as well as higher frequency bands but poor isolation is observed for bottom located antenna elements. However, in the case of data and read mode, top as well as bottom located MIMO antenna provides good impedance matching because the antenna coverage by users body is less compared to the talk mode resulting in less reflection losses and antennas provide above said operating bands and isolation between antenna elements is also well below -10 dB over entire operating bands. The variations of *S*-parameters for the data mode and read mode are shown in Fig. 6.11(b) and 6.11(c), respectively.

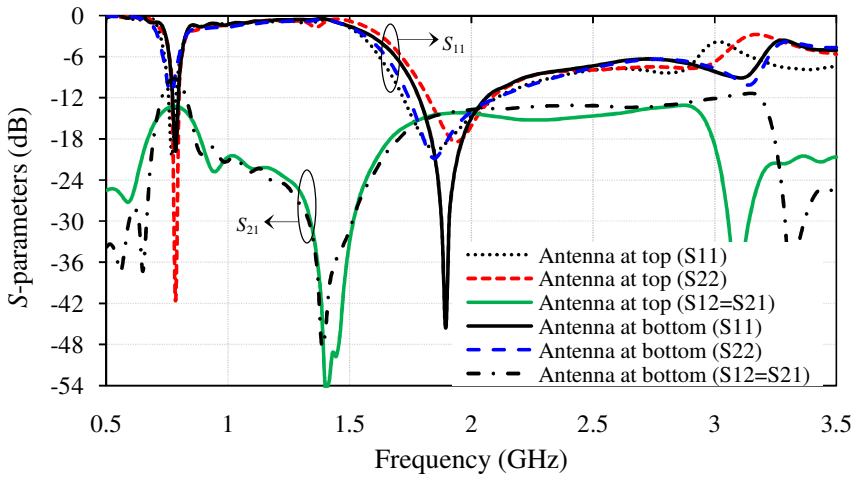

(a)

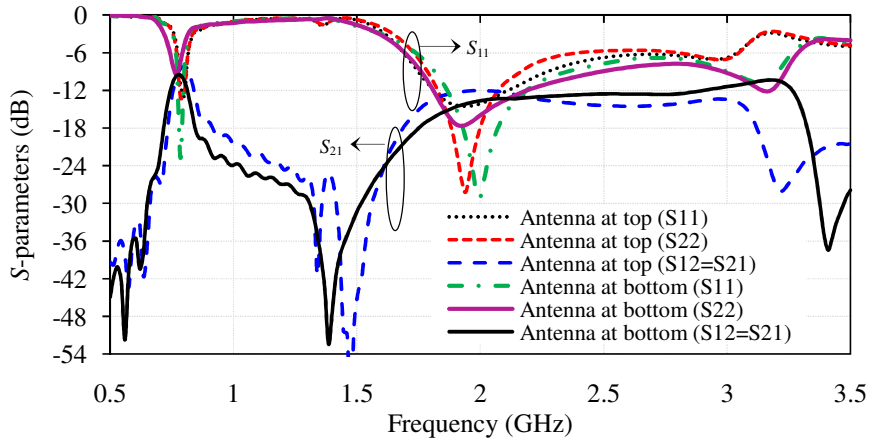

(b)

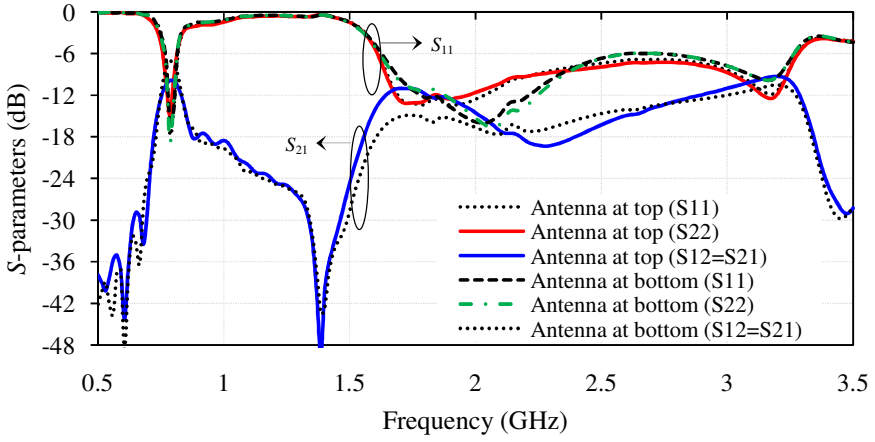

(c)

Figure 6.11: Variation of *S*-parameters of PMA in the user proximity (a) Talk mode, (b) Data mode, and (c) Read mode.

6.4.3 Analysis of Antenna Performances for Different Configurations

In this section, the performance parameters of PMA i.e., total efficiency, ECC, multiplexing efficiency (ME), and mean effective gain (MEG) are investigated for three different configuration namely, talk mode, data mode, and read mode to test the characteristics of PIFA. All the calculation is done according to the previous section.

6.4.3.1 SAM Head and PDA Hand (Talk Mode)

The variations of total efficiency for each antenna elements are shown in Fig. 6.12(a). It is observed that top located antenna elements show better efficiency compareds to the bottom located antenna elements. This is because of the bottom part of the thumb or tip of the little finger which is nearest to the bottom located antenna elements. Whereas efficiency of bottom located antenna elements is not equal due to the asymmetric coverage of antenna elements with user's body and values are low compare to the top located antenna elements. For top located antenna elements, efficiency of both antenna elements (Ant. 1 and Ant. 2) approximately same and it is found that 7% at LTE700 frequency band and varies 20% to 24 % at WWAN band.

By utilizing the formula which have been discussed, ECC is calculated and shown in Fig. 6.12(b). The correlation for bottom located MIMO elements is

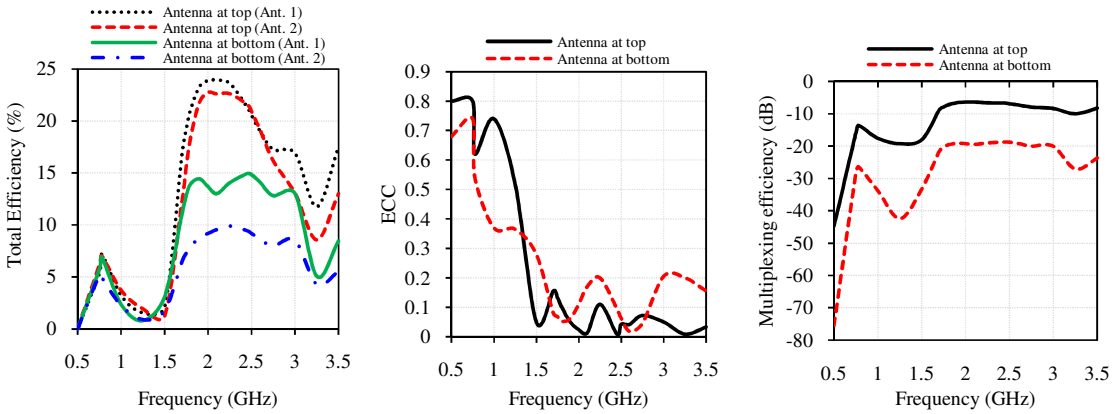

Figure 6.12: (a) Total efficiency, (b) ECC, and (c) Multiplexing efficiency, of the SAM Head and PDA Hand (Talk mode) for PMA.

slightly higher than the top located. This is mainly due to the bottom located MIMO antenna system covered by large human body. However, the ECC is well below 0.5 over the entire operating band for both cases.

The ME of different antenna elements are calculated and shown in Fig. 6.12(c). As expected due to higher efficiency and lower correlation for the top located antenna elements has better multiplexing efficiency than the other combination of the antennas.

In addition to the above parameters, MEG is also an important diversity parameter to study the effect of the user's body. From the Table 6.4, it is observed that MEG decreases in all frequency bands for talk mode either antenna placed at top or bottom. The change of the MEG at different port in user proximity is due to the asymmetrical user body coverage around the antenna elements. However, the ratio of MEG is close to unity, which satisfies the equality criterion for the MIMO antenna.

6.4.3.2 PDA Hand (Data Mode)

The total efficiency for the data mode is shown in Fig. 6.13(a). It is observed that each of the top located antenna elements show approximately same efficiency whereas efficiency variation for bottom located antennas is different which is due to index finger placed approximately symmetrical with respect to the both antenna elements which are placed on top of the mobile circuit board. In the case of bottom located antenna, bottom of thumb and middle finger covers larger area of antennas resulting in lower efficiency is observed. However, efficiency is 27% at LTE700 frequency band and varies between 37 % to 48 % at WWAN band for top located antennas.

The calculated values of envelope correlation coefficient are shown in Fig. 6.13(b). It is observed that ECC's characteristic of data mode at higher frequency is same as talk mode and values are lower than that. The ECCs of data mode are lower than talk mode over entire operating bands. Although, the top located MIMO elements show lower correlation than bottom located antenna elements.

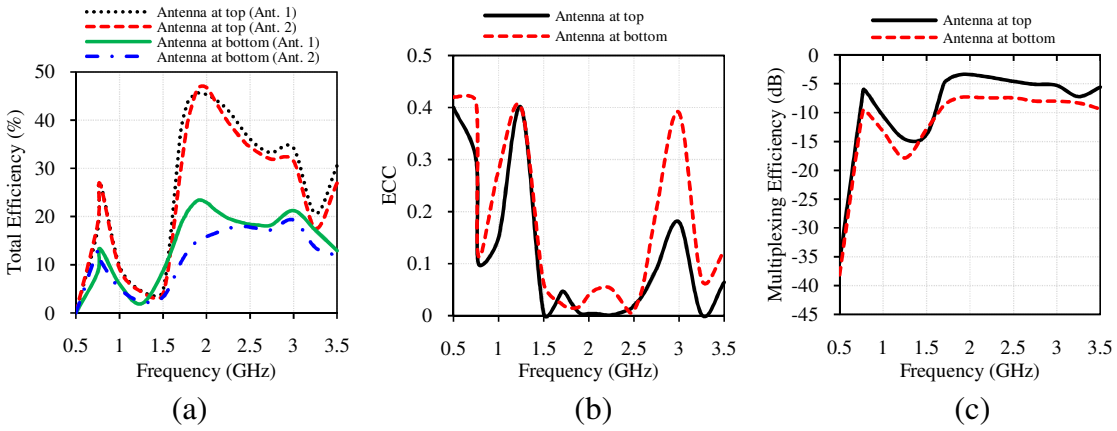

Figure 6.13: (a) Total efficiency, (b) ECC, and (c) Multiplexing efficiency, of the PDA Hand (Data mode) for PMA.

The multiplexing efficiency is also given in Fig. 6.13(c). It can be observed that ME is better for top located antenna in the higher band due to the lower correlation and higher antenna efficiency. Whereas at lower frequency, it shows small variation because variation of ECCs are almost equal for top as well as bottom located antenna.

The variations of MEGs for data mode can be observed from Table 6.4. It is noticed that the dorp of MEG is from 2 dB to 3dB at all the frequencies in comparison to the free space MEGs. Meanwhile the drop of the MEGs for bottom located antennas are more compared to the top located antenna. However, the ratio of MEG is close to unity, which satisfies the equality criteria for the two antennas.

6.4.3.3 Dual Hand (Read Mode)

The variation of total efficiency in the presence of dual hand is shown in Fig. 6.14(a). It is observed that variation of total efficiency of each antenna elements which are placed either top or bottom of the mobile circuit board is approximately same. It is found that efficiency at lower frequency is about 22% whereas at higher frequency it varies between 29% to 48%.

Correlations between the signals are given in terms of ECC which is shown in Fig. 6.14(b). It is found that at lower frequency, ECC for bottom located antenna

is lower that top whereas at higher frequency it is almost equal. However, the values of ECC over operating bands are well below 0.5, which meet the diversity criteria.

The calculated values of ME based and total efficiency and ECCs are shown in Fig. 6.14(c). It is noticed that due to equal total efficiency at all frequency the calculated values of ME is almost equal for top and bottom positioned antenna elements.

The values of MEG for read mode is given in Table 6.4. It is found that variation of MEG for top and bottom placed antenna is approximately similar to the data mode and drop of MEG is also having same nature. The ratio of MEG nearly equal to unity which follow the diversity condition.

6.4.4 Total Radiated Power (TRP) Analysis

The TRP is calculated of PMA similar to the PIFA which has already been discussed in previous chapter (Chapter 5). In the case of multi element MIMO system, the TRP is calculated for each element of MIMO antenna system and named as TRP1 and TRP2 for Ant. 1 and Ant. 2, respectively for top and bottom location of the antenna elements over mobile circuit board. The TRPs are calculated for above three cases namely, talk mode, data mode, and read mode including free space are given in Table 6.5. It is ascertained that in the case of free space, TRP of Ant. 1 and Ant. 2 are same due to the uniform environment

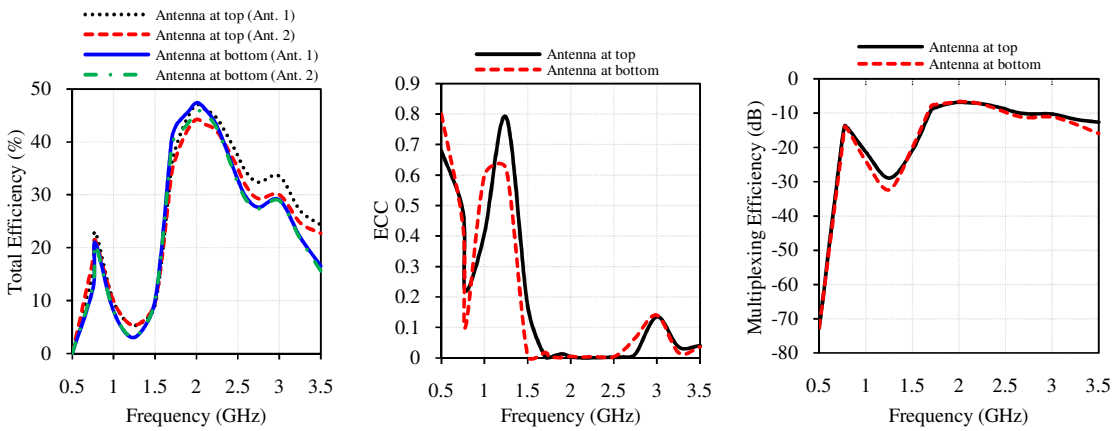

(a) (b) (c)

Figure 6.14: (a) Total efficiency, (b) ECC, and (c) Multiplexing efficiency, of the Dual Hand (Read mode) for PMA.

Table 6.4: Variations of MEG in different user proximity for PMA.

Frequency (GHz)		Antenna at Top		Antenna at Bottom	
		MEG 1	MEG 2	MEG 1	MEG 2
0.777	Free space	-9	-8.9	-9	-8.9
	Talk mode	-6.9	-8.4	-3.15	-2.3
	Data mode	-7.8	-7.8	-6	-4.4
	Read mode	-7.4	-7	-7.6	-7.6
1.9	Free space	-7.8	-7.8	-7.8	-7.8
	Talk mode	-3.7	-5.2	-5.1	-2.8
	Data mode	-5.6	-7.6	-5.2	-2.2
	Read mode	-6.8	-7	-4.9	-4.8
2.1	Free space	-7.2	-7.2	-7.2	-7.2
	Talk mode	-3.5	-4.7	-3	-3.4
	Data mode	-5.45	-7.4	-4.9	-5.8
	Read mode	-7.1	-6.9	-6	-6.1
2.5	Free space	-7.4	-7.4	-7.4	-7.4
	Talk mode	-3.8	-5.2	-5.2	-4.3
	Data mode	-5	-6.4	-4.8	-6.9
	Read mode	-7	-6.9	-6.2	-6.3

Table 6.5: Variations of TRP in different user proximity for PMA.

Frequency (GHz)		Antenna at Top		Antenna at Bottom	
		TRP 1	TRP 2	TRP 1	TRP 2
0.777	Free space	23.4	23.4	23.4	23.4
	Talk mode	13.6	14.8	15.4	14
	Data mode	21.3	21.3	18.2	17.4
	Read mode	20.6	20.3	20.2	20.1
1.9	Free space	26.5	26.5	26.5	26.5
	Talk mode	19.7	19.8	18.6	16.5
	Data mode	23.6	23.7	20.7	18.7
	Read mode	23.5	23.5	23.5	23.3
2.1	Free space	26.2	26.2	26.2	26.2
	Talk mode	20.8	20.5	18.1	16.8
	Data mode	23.4	23.4	20.3	19.2
	Read mode	23.6	23.6	23.6	23.5
2.5	Free space	26	26	26	26
	Talk mode	19	19.8	18.7	16.5
	Data mode	22.5	22.4	19.6	19.5
	Read mode	22.7	22.4	22.1	22.1

around the MIMO antenna elements. Due to the low reflection loss and high total efficiency the TRPs in free space is high i.e. more than 23 dBm. When we implement proposed antenna in real scenario of talk mode, data mode, and read mode, the TRP decreases. For the bottom position, lower TRP is observed, this is because of the larger body coverage and absorption of the power in head and hand phantom. It is also observed that the maximum TRP is occurring in the case of dual hand and minimum TRP occurring in the case of talk mode because area covered by user body is maximum in the case of talk mode and minimum in the case of dual hand.

Further, the loss of power in the presence of user body can be understood with bar chart. The loss of power in bar chart at different frequencies are given in Fig. 6.15. It is interestingly noticed that the bottom positioned antenna shows maximum power loss i.e. 10 dBm for talk mode, 6 dBm for data mode and 2 dBm – 4 dBm for dual hand mode. In the case of top located antenna elements, it is

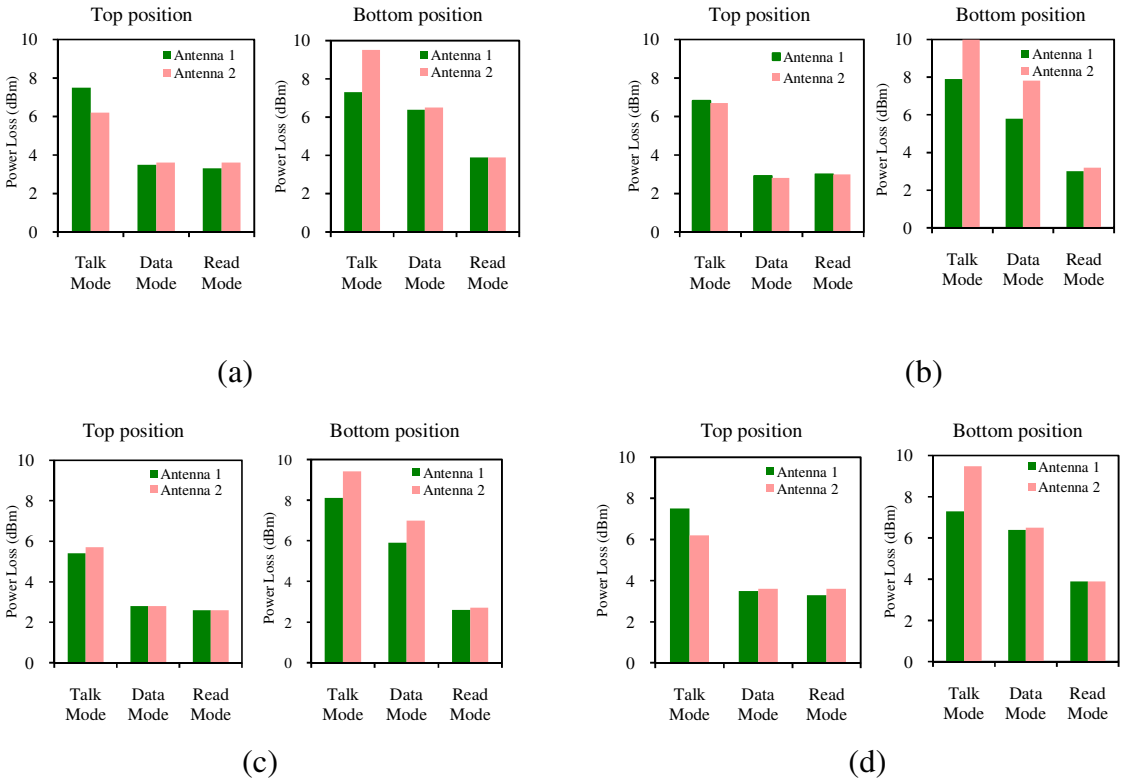

Figure 6.15: Variation of power loss in user proximity at different frequencies of PMA (a) 0.777 GHz, (b) 1.9 GHz, (c) 2.1 GHz, and (d) 2.5 GHz.

found that approximately 8 dBm for talk mode, 3 dBm – 4 dBm for data mode and 2 dBm – 3 dBm for read mode. However, the ranking of the power loss in the user proximity at all the frequencies and for both positions is talk mode, data mode, and read mode. So the higher TRP of top located antenna can significantly improve the call performance of the handset in a weak signal area.

6.4.5 Specific Absorption Rate (SAR) Analysis

To radiation from PMA can be evaluated by SAR, which represent the time rate of microwave energy absorption inside the tissue. The simulation setup for SAR calculation is given in previous chapter (Chapter 5) according to CTIA. The SAR values of Ant. 1 and Ant. 2 are investigated according to the CTIA standard [CTIA Report (2005)] (SAM head and cheek touch). The American standard (FCC) postulate 1.6 W/kg average 1g tissues, while the European standard postulate 2 W/kg average over 10g tissues. The stimulated power for SAR calculation is 24 dBm at lower frequency (0.777 GHz) and 21 dBm for higher frequency (1.9 GHz, 2.1 GHz, and 2.5 GHz). The calculated values of SAR ig given in the Table 6.6. It is observed that the top located antena having larger SAR values compare to the bottom located antenna this is due to the distance difference between antenna and head phantom. The top located antenna is exaclty at 5mm distance form the head phantom whereas bottom located antenna is having larger distance from human head phantom compare to the top located antenna. It is also observed that the SAR is less for both the standard because the antenna is covered with in plastic box. And also found that for both the position, SAR values of Ant. 1 and Ant. 2 is somewhat different because human head phantom is not planar. But from the table it can be concluded that for both the position, values of SAR satisfy the criteria of FCC and European standard.

Further, when the dual antenna operate simultaneously, FCC standard, the value of SPLSR is utilized to evaluate the SAR performance [FCC Report (2008)]. In the calculation of SPLSR, the SAR1 and SAR2 are related to Antenna 1 and Antenna 2, respectively. The separation distance of the two SAR peaks and values of SAR are calculated using CST MWS simulation software. The testing

power for SAR calculation is 24dBm for LTE frequency band (0.777 GHz)) whereas 21dBm for WWAN frequency band (1.9 GHz, 2.1 GHz, and 2.5 GHz) [CTIA Report (2005)]. The calculated values of SPLSR are given Table 6.7. It is observed that the calculated values of SPLSR are well below the defined limit by FCC i.e. 0.3 for top as well as bottom located MIMO antenna. However, bottom located MIMO configuration shows lower SPLSR than top position due to the larger distance between antenna and human head phantom for bottom position.

Table 6.6: SAR values for head phantom due to PMA.

Top Position					
Antenna ↓ / Frequency →		0.777 GHz	1.9 GHz	2.1 GHz	2.5 GHz
Ant. 1 (W/kg)	FCC	0.5	0.68	0.71	0.45
	European	0.34	0.4	0.42	0.25
Ant. 2 (W/kg)	FCC	0. 68	1.3	0.96	0.69
	European	0.45	0.39	0.54	0.39
Bottom Position					
Ant. 1 (W/kg)	FCC	0.36	0.37	0.34	0.23
	European	0.28	0.24	0.21	0.14
Ant. 2 (W/kg)	FCC	0.43	0.39	0.36	0.29
	European	0.34	0.26	0.22	0.17

Table 6.7: Calculated values of SPLSR for planar monopole MIMO antenna.

Top Position								
Distribution of SAR over 1-g tissue					Distribution of SAR over 10-g tissue			
Freq. (GHz)	SAR_1 (W/kg)	SAR_2 (W/kg)	Separation distance b/w SAR peaks (D) unit in centimetre (cm)	SPLSR $=\frac{(SAR_1+SAR_2)}{D}$ (W/kg/cm)	SAR_1 (W/kg)	SAR_2 (W/kg)	Separation distance b/w SAR peaks (D) unit in centimeter (cm)	SPLSR $=\frac{(SAR_1+SAR_2)}{D}$ (W/kg/cm)
0.777	0.5	0.68	3.9	0.3	0.34	0.45	2.4	0.3
1.9	0.68	1.3	6.8	0.29	0.4	0.39	4.3	0.18
2.1	0.71	0.96	6.68	0.25	0.42	0.54	3.5	0.27
2.5	0.45	0.69	4.2	0.27	0.25	0.39	3.2	0.2
Bottom Position								
0.777	0.36	0.43	2.7	0.29	0.28	0.34	2.1	0.29
1.9	0.37	0.39	2.5	0.3	0.24	0.26	2.4	0.21
2.1	0.34	0.36	4.2	0.16	0.21	0.22	1.8	0.24
2.5	0.23	0.29	6	0.087	0.14	0.17	3.3	0.09

6.6 Summary

A planar, printed MIMO antenna for LTE mobile handset is demonstrated. The dual-antenna system, comprises of two symmetrical antenna elements, are printed on PCB of mobile phone. Each antenna element consists of coupled-fed loop antenna. The application platform of the planar monopole MIMO antenna is LTE700, GSM1700, GMS1800, UMTS, Wi-Fi, Bluetooth, LTE2300, and LTE2500 bands for the 2G/3G/4G mobile terminals. A protruded ground plane is used to enhance the isolation at higher frequency side. With the help of protruded ground plane isolation at higher frequency band is achieved well below -10 dB. The proposed diversity antenna is also analysed in the presence of user proximity. The diversity parameters are calculated in free space as well as user proximity and results satisfy the diversity criterion. The calculated values of SAR on the human head phantom are well below the defined standard limit. The results of *S*-parameters, radiation patterns, antenna efficiency, ECC, MEG, and EDG are presented. All the results indicate that the proposed MIMO antenna system is a potential candidate for portable usages to combat multipath fading practical applications and more promising for slim LTE/WWAN smart applications.

After analysing the performance study of the proposed antenna in both free space as well as user proximity with mobile environment, the entire investigations carried out in various chapters is summarized in the last chapter of summary and conclusion which is given in the following chapter seven.